ELSEVIER

Biochemical Pharmacology 64 (2002) 711–721

Biochemical Pharmacology

Expression and activity of the DNA repair enzyme uracil DNA glycosylase during organogenesis in the rat conceptus and following methotrexate exposure *in vitro*

Robert K. Vinson, Barbara F. Hales*

Department of Pharmacology and Therapeutics, McGill University, 3655 Promenade Sir-William-Osler, Montréal, Que., Canada H3G-1Y6

Received 29 November 2001; accepted 14 February 2002

Abstract

Uracil incorporation into DNA occurs under conditions that limit thymidine biosynthesis; uracil is removed by two isoforms of uracil DNA glycosylase (UNG; EC 3.2.2.3), UNG1 and UNG2. We hypothesize that UNG is important in protecting the mid-organogenesis stage [gestational day (GD) 10–12] rat conceptus against conditions that limit thymidine biosynthesis. Transcripts for both UNG isoforms were expressed highly in the yolk sac and embryo, increasing over 400% in the embryo between GD11 and 12. GD10 and 11 yolk sacs showed the highest levels of putatively active UNG2 protein, with little UNG1 protein. Moderate levels of UNG2 and UNG1 proteins were found in the embryo on GDs 10 through 12; no significant increase in either protein occurred on GD12. UNG activity was higher in yolk sac than embryo on GDs 10 and 11, mirroring protein levels. Exposure to the teratogen methotrexate (MTX) leads to nucleotide pool imbalance, uracil incorporation into DNA, and genotoxic stress-induced cell death. Concentration-dependent decreases in developmental growth parameters, decreased yolk sac vasculature, and malformations such as kinked tail and retarded limb development were observed in embryos exposed to MTX (0.5, 2.5, or 5 μM). *UNG* transcripts were elevated 30–40% in both yolk sac and embryo after a 6-hr culture with 0.5 μM MTX; however, protein expression and activity were unaffected. Thus, MTX exposure caused malformations but did not modify UNG protein expression or activity, indicating an inability to increase the removal of MTX-induced genotoxic damage. Furthermore, UNG expression was developmental stage- and tissue-specific; the discrepancy between transcript and protein levels suggests post-transcriptional regulation.

Keywords: DNA repair; Methotrexate; Organogenesis; Rat conceptus; Teratogen; Uracil DNA glycosylase

1. Introduction

The ability to remove misincorporated nucleotides is crucial to ensure genomic integrity, particularly during development due to the specific program and timing of gene expression required for proper embryonic growth. Genotoxic stress has the ability to alter cellular function and viability drastically. Both dietary folic acid deficiency and exposure to MTX induce genotoxic damage and malformations. Folic acid is a water-soluble B vitamin, and is an essential cofactor for the enzyme DHFR [1]. Folic acid deficiency during pregnancy results in NTDs, congenital heart defects, renal and urinary tract defects, limb malformations, and facial clefts (palate and lip) in the newborn [2]. NTDs, such as spina bifida and anencephaly, occur with a frequency of one per 1000 births in the United States, and are among the most common forms of birth defects [3] and causes of perinatal mortality observed [2]; in the United Kingdom, 15% of perinatal deaths are attributed to NTDs [4]. MTX, a structural analog of folic acid and a potent inhibitor of DHFR, causes malformations that are similar to those induced by folic acid deficiency. The teratogenic effects of MTX have been reported in rats [5], mice [6], rabbits [7], cats [8], and humans [9,10].

Folic acid is required for the synthesis of products for the one-carbon metabolic pathway [11]. DHFR catalyzes the formation of 5,10-MTHF, an essential cofactor for *de novo* synthesis of purine bases and the pyrimidine base

* Corresponding author. Tel.: +1-514-398-3610; fax: +1-514-398-7120.
E-mail address: bhales@pharma.mcgill.ca (B.F. Hales).

Abbreviations: 5,10-MTHF, 5,10-methylenetetrahydrofolate; APE, AP endonuclease; aRNA, antisense RNA; ATA, aurintricarboxylic acid; DHF, dihydrofolate; DHFR, dihydrofolate reductase; GD, gestational day; MTX, methotrexate; NTDs, neural tube defects; TBE, Tris-buffered EDTA; TBS, Tris-buffered saline; UGI, uracil DNA glycosylase inhibitor; UNG, uracil DNA glycosylase.

0006-2952/02/$ – see front matter
PII: S0006-2952(02)01252-2

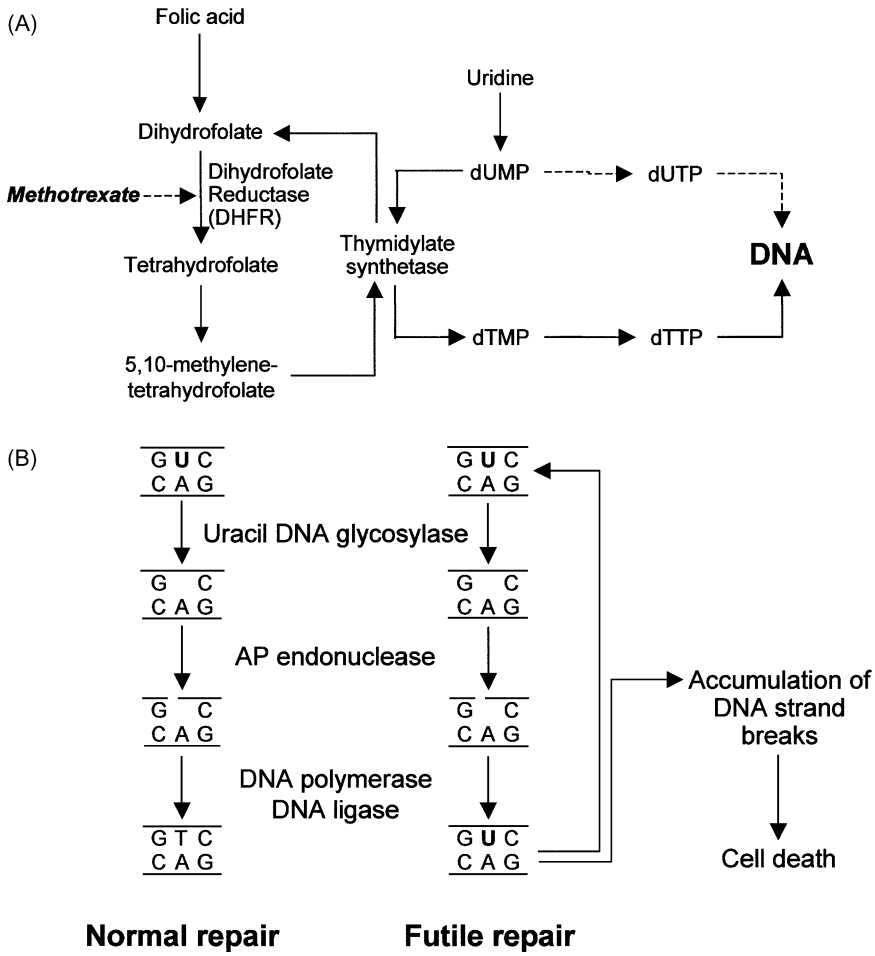

Fig. 1. (A) Folic acid one-carbon and thymidine nucleotide biosynthetic pathways. The consequence of inhibition of DHFR by MTX, leading to dUTP incorporation into DNA, is shown by the dashed line. (B) UNG repair pathway under normal conditions (left) or during conditions of thymidine depletion (right) leading to futile repair.

thymidine (Fig. 1A). Synthesis of dTMP from dUMP by thymidylate synthetase requires 5,10-MTHF as a methyl donor, yielding DHF, which is then converted back to 5,10-MTHF by DHFR. Both folic acid deficiency and MTX alter the biosynthesis of thymidine: folic acid deficiency depletes 5,10-MTHF levels due to lack of substrate, while MTX depletes 5,10-MTHF via inhibition of DHFR. In both instances, subsequent inhibition of dTMP synthesis leads to an increase in dUMP levels. Under normal cellular conditions, DNA polymerases preferentially utilize dTTP; however, if cellular dUTP pools grow larger than dTTP pools, dUTP is incorporated into DNA due to a lack of substrate specificity in the polymerase nucleotide binding pocket [12]. Uracil incorporation into DNA due to thymidine depletion [13–16] leads to DNA fragmentation and cell death [17]. The loss of cell viability following a dramatic decrease in thymidine levels is termed "thymidineless death" [18]. Concomitant loss of DNA repair capacity occurs, also due to imbalanced nucleotide pools [19].

The teratogenic action of MTX has been demonstrated to be due mainly to the inhibition of DHFR, as transgenic animals expressing an MTX-resistant form of DHFR have decreased incidences of malformations upon MTX exposure [20]. The exact cause of the specific malformations induced by MTX is uncertain. Alterations in tissue structure, haemorrhage, and oedema were observed in sensitive tissues following MTX exposure in mice [21] and rabbits [6].

The DNA base excision repair enzyme UNG is the principal mammalian enzyme that removes misincorporated uracil from DNA. The mammalian *UNG* gene encodes two enzyme isoforms via separate promoters: UNG1, which localizes to mitochondria, and UNG2, which is nuclear in humans [22,23] and both mitochondrial and nuclear in mice [24]. These *UNG* products make up the majority of uracil excision activity in cells [25]. Both isozymes recognize uracil and remove it via a "base-flipping" mechanism [26], cleaving the glycosydic bond to the DNA sugar backbone (Fig. 1B). An APE then removes the ribose moiety from the backbone, DNA polymerase fills in the gap formed, and DNA ligase reconnects the cut ends.

Tissues from adult *Ung* null-mutant mice exhibit levels of uracil in DNA that are elevated over four times those

found in normal cells [24]. Human UNG1 and UNG2 are both expressed highly in proliferative tissues, such as testis, colon, and thymus [27]; the expression of rodent isoforms is also correlated with the proliferative status of the tissue [28,29]. UNG activity, but not transcript or protein levels, has been examined late during rat development [28], but not during mid-organogenesis (GD10–12), a critical period during which time a variety of tissues first begin to differentiate into organ systems.

We hypothesize that UNG is important in protecting the embryo against the consequences of limited thymidine levels during organogenesis. Removal of dUTP from DNA is critical for normal genome function. The role of UNG in preventing uracil incorporation into DNA during development is evident, as both murine *Ung* homologues are expressed during organogenesis [29]. Decreased cellular thymidine levels require the activity of UNG, particularly during cell proliferation or development. The role of UNG in folic acid deficiency-induced birth defects has not been explored. The first goal of this study was to characterize the expression and activity of UNG during mid-organogenesis. Furthermore, we hypothesize that MTX-induced thymidine deprivation may affect UNG expression. To test these hypotheses we have characterized the *UNG* gene and protein expression, as well as activity, in the rat conceptus *in vivo* and examined the consequences of MTX exposure *in vitro* on UNG expression and activity.

2. Materials and methods

2.1. Tissue preparation

Timed-pregnant virgin female Sprague–Dawley rats (200–225 g) were obtained from Charles River Canada and housed in the McIntyre Animal Resource Centre. Food and water were provided *ad lib.*, and animals were exposed to a 14-hr light:10-hr dark cycle. All treatments were in accordance with a protocol approved by the Animal Care Committee of McGill University. GD zero was defined as the morning following mating. On GD10, 11, and 12, uteri were removed, and embryo and yolk sac tissues were dissected immediately and either frozen individually in liquid nitrogen for gene expression analysis or pooled for protein analysis, and stored at -80°.

2.2. Embryo culture

The whole embryo culture model removes any confounding maternal effects that may occur following drug exposure. GD10 conceptuses with an intact yolk sac and ectoplacental cone were cultured for 6, 24, or 44 hr in the presence of vehicle (sterile water) or in the presence of 0.5, 2.5, or 5 μM MTX (Sigma-Aldrich), as previously described [30]. Following culture, embryos were removed and dissected as described above.

2.3. aRNA technique

The aRNA technique was used to examine *UNG* gene expression in individual embryos [31,32], and was performed as previously described [33]. Total RNA from individual samples of embryo and yolk sac was extracted, and mRNA from this pool was converted into cDNA with an oligo(dT) primer attached to the T7 RNA polymerase promoter, reverse transcriptase (Gibco BRL), S1 nuclease (Gibco BRL), T4 DNA polymerase (Gibco BRL), and Klenow fragment (New England Biolabs). aRNA was amplified from the cDNA templates using T7 RNA polymerase (New England Biolabs) and labelled with [α-^{32}P]CTP (10 mCi/mol; Amersham Pharmacia Biotech). Labelled aRNA was hybridized overnight to nylon membranes (Zeta-Probe GT, Bio-Rad) previously slot-blotted with equimolar amounts of cDNAs encoding the *UNG* DNA repair gene isoforms. The membranes were washed in solutions of decreasing stringency, and were exposed overnight to Phosphorimager plates. The linearity and reproducibility of this amplification reaction were determined by trichloroacetic acid precipitation of [α-^{32}P]CTP incorporated into the acid-insoluble fraction.

2.4. Quantification and analysis of aRNA data

Images of the blots were obtained using a STORM Phosphorimager (Molecular Dynamics). Quantification of gene expression was done using ImageQuant 5.0 software (Molecular Dynamics). Data are expressed as the mean percent of *UNG* expression relative to vimentin from the same membrane ± SEM of tissues from five to seven separate GD10–12 samples for *in vivo* results, or four to five separate samples for culture alone or for MTX treatment, each obtained from separate litters. The data are represented relative to the structural protein gene vimentin, as its expression did not change more than 2–4% of the total blot intensity between the different time points and tissues examined (data not shown).

2.5. Protein extraction

Embryonic tissue was sonicated on ice (Vibracell, Sonics & Materials) in RIPA buffer containing a mixture of protease inhibitors (0.2 M phenylmethylsulfonyl fluoride, 10 μg/mL of leupeptin, 3 μg/mL of aprotinin, and 40 μg/mL of bestatin) (Roche Diagnostics), and spun at 12,000 *g* for 10 min at 4°; the supernatant was removed for protein analysis. Protein concentrations were determined by the Bio-Rad Protein Assay. Samples were frozen at -80° until used.

2.6. Western blot analysis

Protein samples (40 μg) were mixed with SDS-loading buffer, boiled for 5 min, centrifuged briefly (14,000 *g* for

10 min at room temperature), and electrophoresed on a 10% SDS–polyacrylamide gel for 2.25 hr at 100 V. Samples were transferred to Hybond-C Super nitrocellulose membranes (Amersham Pharmacia Biotech) at 130 V for 2 hr at 4°. Membranes were dried briefly, washed with TBS plus 0.1% Tween-20 (TBS-T) for 2 × 5 min, and then incubated with TBS-T supplemented with 5% (w/v) non-fat dry milk (5%M-TBS-T) for 1 hr to block non-specific antibody binding. Membranes were washed, then incubated with an anti-UNG antibody (1:5000 final dilution; a gift from G. Slupphaug) in 5%M-TBS-T overnight at 4°. A donkey anti-rabbit (1:2500; Amersham Pharmacia Biotech) secondary antibody conjugated to horseradish peroxidase (HRP) was used to detect specific antibody interactions. Specific antibody binding was visualized with the ECL-Plus Kit (Amersham Pharmacia Biotech) and Hyperfilm ECL (Amersham Pharmacia Biotech). Protein molecular weight determination was done by visualization on the blots of Precision™ prestained protein standards (Bio-Rad) and biotinylated SDS–PAGE broad range standards (Bio-Rad) after incubation for 5 min with a Streptavidin-HRP conjugate (Amersham Pharmacia Biotech) diluted 1:5000 in TBS-T. Adult rat testis and recombinant UNG (New England Biolabs) were used as positive controls. Actin expression was used as a loading control by incubating membranes with an anti-actin antibody (1:500; Santa Cruz) for 3 hr at room temperature (RT) in 5%M-TBS-T.

2.7. DNA substrates for UNG assay

Oligonucleotide substrates were synthesized by the Sheldon Biotechnology Centre (McGill University). The sequences of the oligonucleotides were as follows:

30U: 5′-GGATGGCATGCATGATCC(U)GAG-GCCGCGCG-biotin-3′
30T: 5′-GGATGGCATGCATGATCC(T)GAG-GCCGCGCG-biotin-3′
30compl: 5′-CGCGCGGCCTCAGGATCATGCATGC-CATCC-3′.

Double-stranded oligonucleotide substrates (ds30U, ds30T) were prepared by annealing equimolar amounts of 30U and 30compl for ds30U, or 30T and 30compl for ds30T, for 5 min at 85°, and allowing them to cool slowly to RT. Annealing efficiency was determined by electrophoresis on a non-denaturing 20% polyacrylamide gel.

2.8. In vitro UNG activity assay

The same tissue extracts used for western blot analysis (20 μg) were incubated with 10 ng oligonucleotide substrate (either ds30U or ds30T) in 20 mM Tris–HCl (pH 8.0), 1 mM EDTA, 1 mM dithiothreitol, 0.1 mg/mL of BSA, and 10 mM $MgCl_2$ in 50 μL final volume. The repair reaction was carried out for 30 min at 37°. Recombinant human APE [10 U; used along with recombinant UNG (10 U) as a positive control] was from Trevigen.

2.9. Denaturing gel electrophoresis

UNG activity assay products (5 μL) were mixed with an equal amount of denaturing loading buffer [8 M urea, 20 mM EDTA, 5 mM Tris–Cl (pH 7.5)], heated for 5 min at 90°, and separated by electrophoresis on a 20% polyacrylamide mini-gel containing 3.9 M urea, 22% formamide, and 1× TBE buffer. Gels were pre-run at 240 V for 1 hr; samples were added and run at 240 V for 50 min in 1× TBE buffer. A 10 bp ladder (Gibco BRL) was used as a sizing standard for visualization of samples under short-wave UV light following ethidium bromide staining of the gel. The samples were blotted onto a Zeta-Probe GT nylon membrane (Bio-Rad) using a Trans-Blot SD semi-dry transfer apparatus (Bio-Rad) running at 210 mA (constant) and 7 V for 10 min in 0.5× TBE buffer. The membrane was baked for 30 min at 80°; then samples were visualized by a Phototope-Star Detection Kit (New England Biolabs), and exposed to Hyperfilm ECL (Amersham Pharmacia Biotech). Quantification of UNG activity was done using a ChemiImager 4000 imaging system (Alpha Innotech) with AlphaEase 3.3b software.

2.10. Statistical analysis

Statistical analyses were done with SigmaStat version 2.03 Windows PC software (SPSS).

3. Results

3.1. UNG gene expression in vivo

Transcripts for both UNG1 (Fig. 2A) and UNG2 isoforms (Fig. 2B) were expressed at high levels relative to vimentin in GD10 to 12 embryo and yolk sac samples. Quantification of these data showed a dramatic 400% increase in both transcript levels on GD12, specifically in the embryo, as compared with GD10 UNG expression.

3.2. UNG protein expression in vivo

To determine whether changes in the steady-state concentrations of the *UNG* transcripts corresponded to differences in protein levels, the expression of both UNG isoforms was examined by western blot analysis (Fig. 3). High levels of the nuclear isoform, UNG2, were observed in the yolk sac. In particular, two specific bands were detected. A higher-MW, phosphorylated species has been observed following western blot analysis, and is believed to be the active form of the isozyme.[1] This band was apparent

[1] G. Slupphaug, personal communication. Cited with permission.

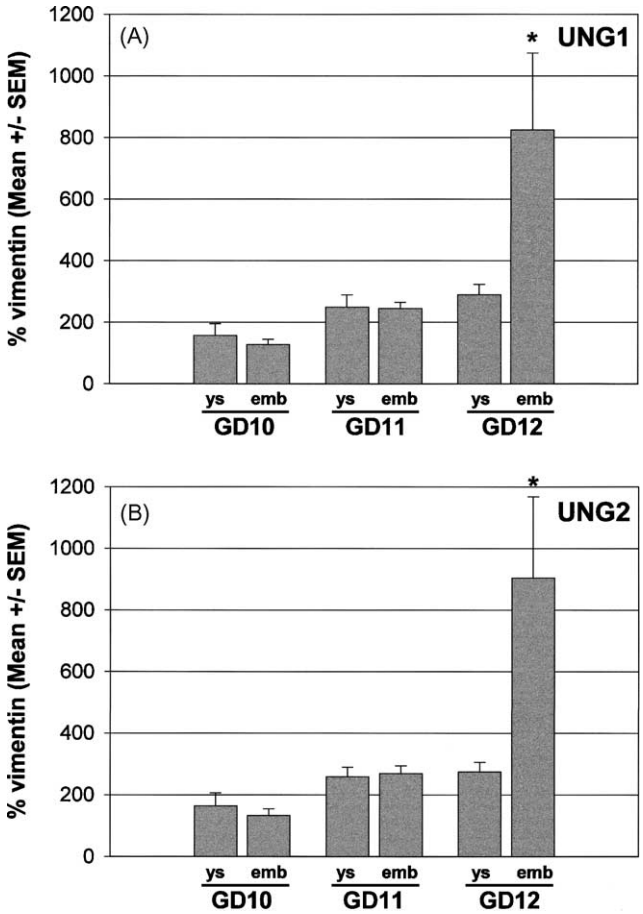

Fig. 2. Quantitative analysis of (A) *UNG1* and (B) *UNG2* transcript expression profiles in the rat conceptus during organogenesis. Gestational-age and tissue-dependent gene expression was seen during mid-organogenesis. *UNG* gene expression was analyzed from arrays probed with aRNA samples from yolk sac (ys) or embryo (emb) tissues from GD10 to GD12. Data are expressed as the mean percent of vimentin expression ± SEM of tissue from 5 to 7 separate GD10–12 yolk sac and embryo samples obtained from different litters. Key: (∗) significantly different from GD10 and 11 ($P < 0.05$) as determined by ANOVA and Tukey's test.

on GDs 10 and 11 in the yolk sac, but not on GD12. In contrast, the embryo from GD10 to 12 displayed only the higher-MW UNG2 band, at consistently lower levels than the yolk sac. Levels of the mitochondrial isoform, UNG1, were moderate in the embryo at all three time points; however, little or no UNG1 was observed in yolk sac samples. An additional, uncharacterized band appeared slightly above that for UNG1, which may be a modified form of the enzyme. Adult rat testis, used as a positive control, showed both UNG1 and UNG2 bands, as well as a yet uncharacterized lower MW band; recombinant *Escherichia coli* UNG ran as the expected single band.

3.3. UNG enzyme activity in vivo

To determine the capacity of the conceptus to remove uracil from DNA, tissue samples were incubated with a double-stranded 30-mer oligonucleotide containing a single uracil residue at position 19 (ds30U); UNG activity causes the substrate DNA band at 30 bp to disappear, forming an 11 bp fragment due to the removal of uracil by UNG and the subsequent cleavage at the AP site by APE. UNG activity assay results are shown in Fig. 4. At all three developmental time points examined (GD10–12), both yolk sac and embryo samples had the ability to excise uracil from DNA. GD10 and 11 yolk sac samples had dramatically reduced amounts of the substrate 30-mer oligonucleotide (Fig. 4, top photograph) with increased amounts of the 11 bp fragment, indicating a high uracil removal ability. GD12 yolk sac had a much-reduced rate of excision of the substrate, and was similar to the GD12 embryo. Quantification of the intensity of the 11 bp fragment is shown graphically below the gel in Fig. 4. The high activities found in GD10 and 11 yolk sac samples mirrored the high protein levels found in these tissues by western blot analysis (Fig. 3).

Additional bands, between the 30 bp full-length substrate and the 11 bp cleavage product, were visible in the GD10 and 11 yolk sac samples. The addition of 100 μM ATA, an inhibitor of nucleases [34,35], to the reaction mixture caused the additional bands to disappear (data not shown), with a concomitant decrease in the intensity of the 11 bp fragment and an increase in the intensity of the 30 bp band, indicating that ATA also inhibits UNG activity. Addition of a specific bacteriophage UNG inhibitor,

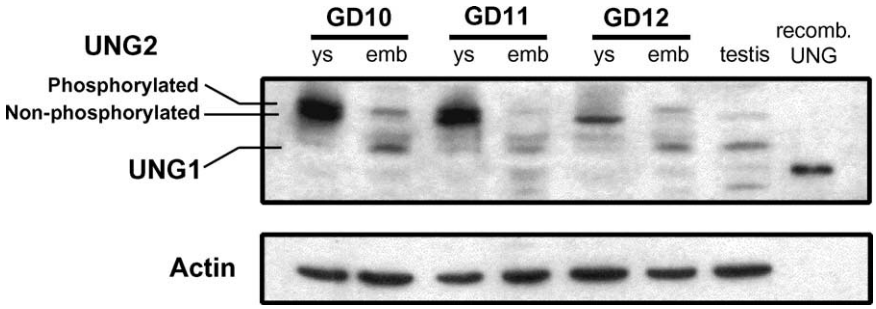

Fig. 3. Western blot analysis of the expression of UNG1 and UNG2 proteins during organogenesis *in vivo*. Gestational-age and tissue-dependent protein expression was seen during mid-organogenesis. UNG2 appeared as two bands (putatively phosphorylated and non-phosphorylated). Rat testis extract and recombinant UNG protein were used as positive controls. Actin was used as a loading control. This experiment is representative of results from 3 different sets of tissue samples from separate litters. ys, yolk sac; emb, embryo.

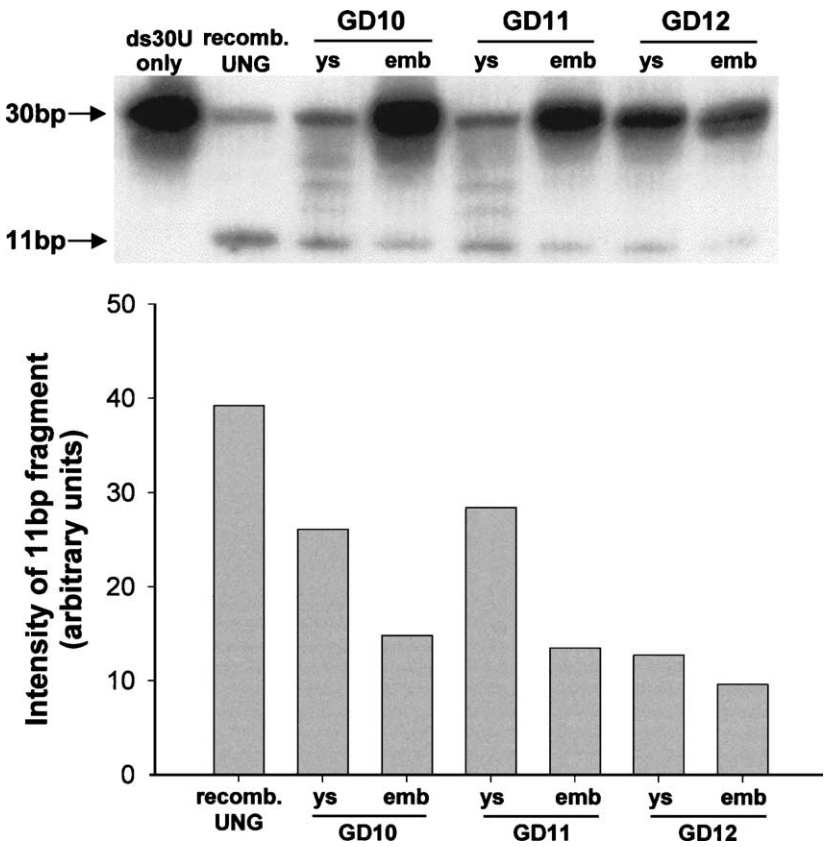

Fig. 4. UNG activity in the rat conceptus during organogenesis. Repair reaction products were separated on a 20% denaturing polyacrylamide gel (top photograph). The first lane contains 2 ng ds30U oligonucleotide only. Subsequent lanes are aliquots of reaction samples containing 10 ng ds30U oligonucleotide and: 10U each recombinant UNG and APE (recomb. UNG lane) or GD10–12 yolk sac and embryo tissue extracts. A semi-quantitative analysis of the assay is shown below the photograph. Data are represented as the intensity of the 11 bp oligonucleotide band. This experiment is representative of results from 3 different sets of tissue samples from separate litters. ys, yolk sac; emb, embryo.

UGI (New England Biolabs) [36], did not remove the additional bands, indicating that they were not due to UNG activity (data not shown). The additional bands remained when an oligonucleotide containing a thymidine, instead of a uracil, at position 19 (ds30T) was used in the reaction assay (data not shown). Therefore, the additional bands are not due to UNG activity and are not specific for uracil-containing DNA. Inhibition by ATA suggests that they may be due to other DNA nucleases present in the yolk sac on GD10 and 11.

3.4. MTX teratogenicity in vitro

To assess the *in vitro* teratogenicity of MTX during mid-organogenesis, GD10 embryos were cultured for 24 or 44 hr with 0.5, 2.5, or 5 μM MTX, then examined by using the Brown-Fabro scoring system [37], and by counting somite numbers. Following culture for 24 hr, a concentration-dependent decrease in embryonic growth was observed (Fig. 5; 2.5 μM MTX not shown).

Decreased yolk sac vasculature and malformations such as kinked tails, growth retarded limbs, blebs, eye defects, and a general decrease in overall embryo size were observed even at the lowest concentration used (0.5 μM MTX; Fig. 5B) compared with control embryos (Fig. 5A); embryo defects were even more severe at the highest concentration (5 μM MTX; Fig. 5C). The developmental retardation was quantitated as a decrease in both the Brown-Fabro scores (Fig. 6A) and somite numbers (Fig. 6B) with all three concentrations of MTX. Both developmental parameters were decreased further following a 44-hr culture with MTX (data not shown).

3.5. UNG gene expression following MTX exposure

The effect of MTX exposure on *UNG* gene expression was examined following short-term (6 hr) culture *in vitro* (Fig. 7). Low-concentration (0.5 μM) MTX induced a 30–40% increase in transcripts for both UNG isoforms in both yolk sac and embryo for UNG1, and in the yolk sac for UNG2. Exposure to 5 μM MTX had no significant effect on *UNG* transcript levels.

3.6. UNG protein expression following MTX exposure

To determine if UNG protein levels increased in parallel with gene expression, conceptuses were cultured with MTX for 6 hr and examined for UNG1 and UNG2 protein

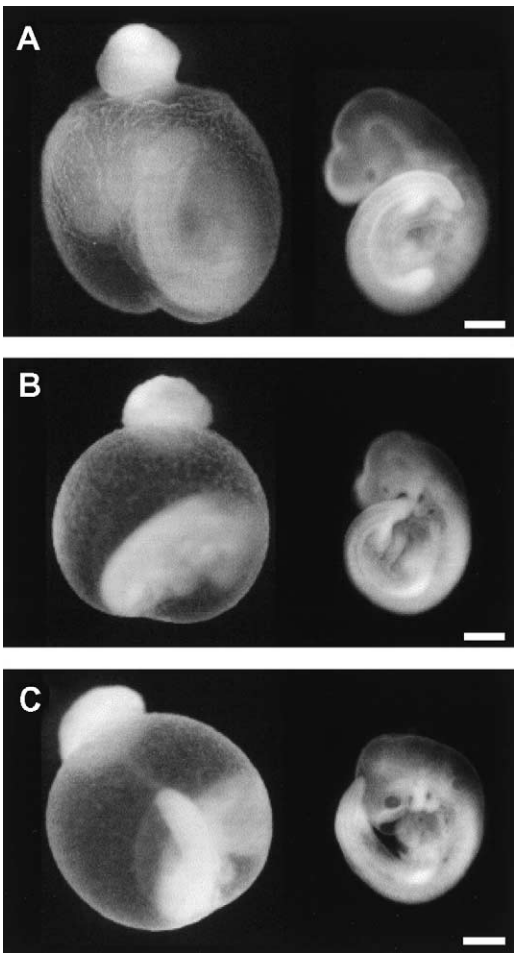

Fig. 5. Dark-field photographs of embryos with intact yolk sacs (left) or with yolk sacs removed (right) following 24-hr *in vitro* embryo culture with (A) vehicle alone, (B) 0.5 μM MTX, or (C) 5 μM MTX. Decreased yolk sac vasculature, retarded limb development, blebs, eye defects, and an overall decrease in size was seen following exposure to MTX. All pictures are to the same scale (bar = 1 mm).

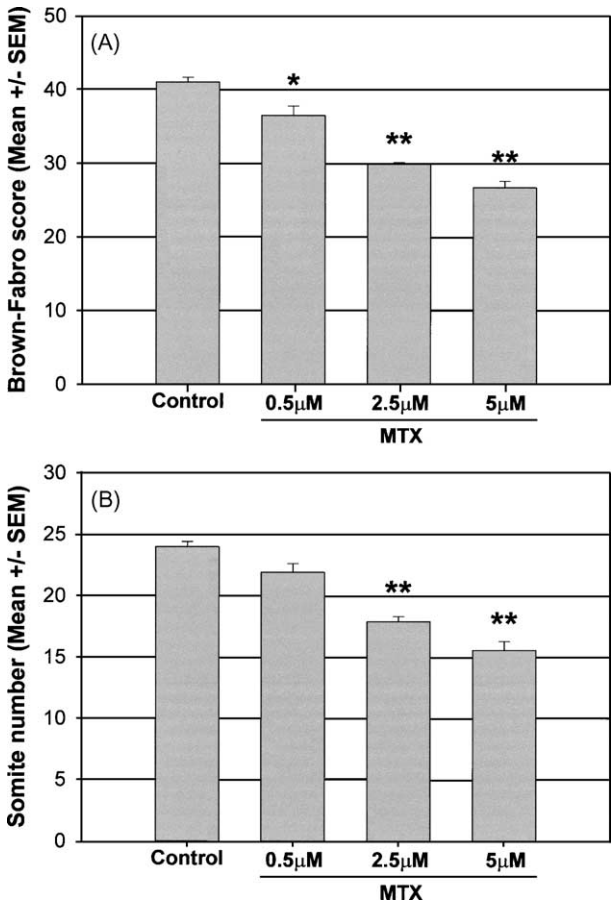

Fig. 6. Quantification of developmental parameters following *in vitro* culture with vehicle alone or MTX (0.5, 2.5, or 5 μM). (A) Brown-Fabro scores and (B) somite numbers following a 24-hr culture. A concentration-dependent decrease in both parameters was seen following MTX exposure. Data are expressed as the means ± SEM from 11–13 embryos. Key: (∗) significantly different from control or (∗∗) control and 0.5 μM MTX ($P < 0.05$) as determined by ANOVA on Ranks followed by Dunn's post-hoc test (Brown-Fabro scores) or by one-way ANOVA followed by Tukey's test (somite numbers).

expression (Fig. 8). Unlike the *in vivo* results, UNG1 was present in equal amounts in the yolk sac and embryo of cultured embryos. As in the *in vivo* results, both non-phosphorylated and phosphorylated forms of UNG2 were found at equivalent levels in the yolk sac in control samples, while the embryo expressed only the active phosphorylated UNG2 form; UNG2 protein concentration did not change following MTX exposure. After MTX exposure for 24 hr (data not shown), similar concentrations of both UNG isozymes were found, compared to exposure for 6 hr, in either yolk sac or embryo.

3.7. UNG enzyme activity following short-term culture with MTX

UNG enzyme activities following culture with MTX for 6 hr are shown in Fig. 9. Yolk sac from control embryos had slightly higher activity levels than MTX-exposed tissues. In addition, all three yolk sac samples showed additional bands between the substrate and cleaved oligonucleotide product. Both yolk sac and embryo proper, exposed to either concentration of MTX, had similar activity levels.

4. Discussion

This study provides evidence for the differential expression and activity of the major uracil removing glycosylases during mid-organogenesis in the rat conceptus. Steady-state concentrations of the transcripts for both UNG isoforms were high in the conceptus, in agreement with a previous study which showed that both UNG isoforms are expressed in murine embryos during mid-gestation [29]; these data suggest an increased need to remove uracil from DNA during this period of development. In fact, transcripts for UNG1 and UNG2 are among the highest-expressed DNA repair transcripts from any repair pathway in the rat

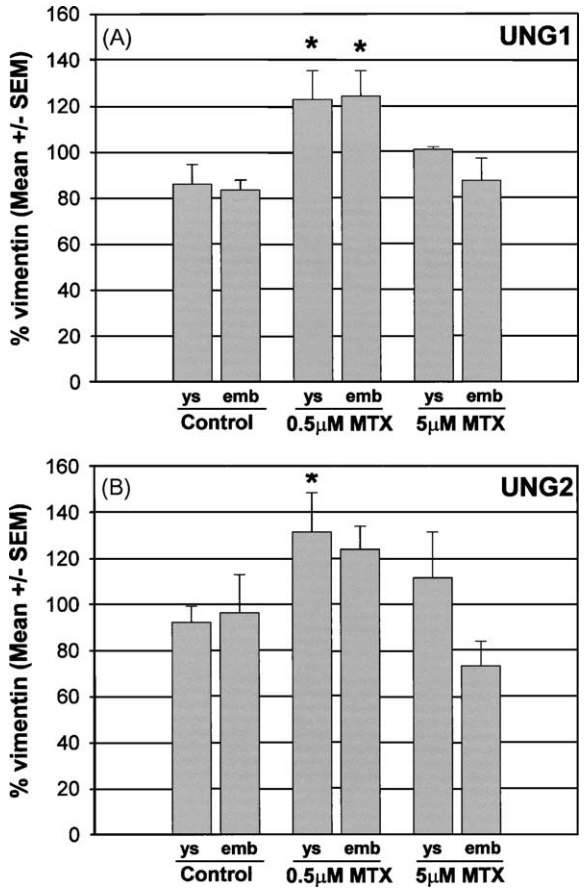

Fig. 7. Expression of *UNG* transcripts for (A) UNG1 and (B) UNG2 following a 6-hr culture with vehicle alone or with MTX (0.5 or 5 μM). *UNG* gene expression was analyzed from arrays probed with aRNA samples from yolk sac (ys) or embryo (emb). MTX increased gene expression following a low concentration, but not a high concentration, exposure. Key: (∗) significantly different from control ($P < 0.05$) as determined by Student's *t*-test with Bonferroni correction.

conceptus during this period of development [33,38]. The high levels of expression of *UNG* during development may indicate the importance of this pathway as a defensive cellular mechanism to ensure that genetic integrity is maintained during a highly proliferative state.

Interestingly, while *UNG* transcript levels increased on GD12, protein levels did not parallel this increase. While *UNG* transcripts were expressed at similar levels, there were distinct differences in the protein concentrations of the two UNG isozymes. In particular, concentrations of nuclear UNG2 were higher than those of the mitochondrial isozyme. As well, there was much greater expression of UNG2 in the yolk sac; the UNG2 apparent in the embryo was exclusively of the higher-MW, putatively phosphorylated variety, which is hypothesized to be the active form of the enzyme. Conversely, UNG1 was expressed at higher levels in the embryo than the yolk sac. Why the yolk sac would require high levels of UNG2, and not UNG1, during development is unknown; perhaps thymidine pools are lower in yolk sac cells, thereby requiring a greater ability to remove misincorporated nucleotides in nuclear DNA.

Further differences between yolk sac and embryo proper with respect to UNG protein levels were found. Higher-MW protein bands were observed via western blot analysis at all three developmental time points examined *in vivo*. These high-MW species have been hypothesized to represent ubiquitinated UNG (see footnote 1). Bands for specific ubiquitinated protein products overlapped those of the higher-MW UNG products, strengthening this hypothesis. While the precise role of ubiquitination of UNG is unknown, ubiquitination is the major method of targeting proteins for degradation, and altering protein turnover rate [39]. Higher protein turnover rates may help to explain the lack of correspondence between transcripts (high levels, particularly on GD12 in the embryo) and protein (low levels). Nilsen *et al*. [29] proposed that *UNG* expression during development is modulated by transcription altering factors, such as MZF-1, which are present during development. Both UNG [40] and MZF-1 [41] are highly expressed in haematopoietic cells; as the yolk sac is the main site of haematopoiesis at this time during development [42], the high concentrations of UNG2 in this tissue may be in haematopoietic cells within this tissue.

Maximal UNG activity was observed previously around birth in the rat [28], although the only pre-natal time point examined in this study was 4 days prior to birth. Nevertheless, several of the organs that were examined had their highest levels of UNG activity before birth, with activity

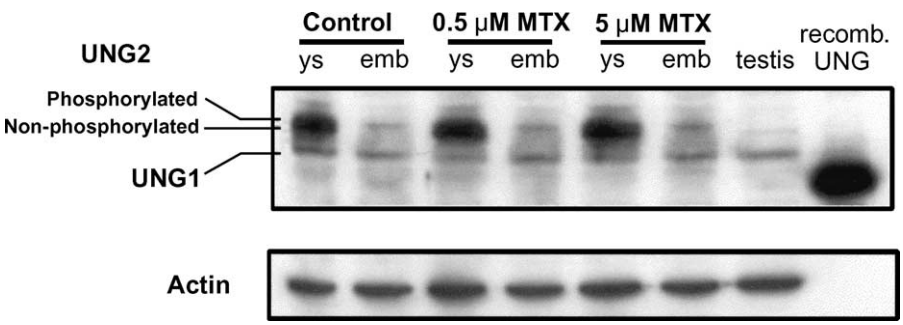

Fig. 8. Western blot analysis of the expression of UNG protein isoforms following a 6-hr culture with either 0.5 or 5 μM MTX to determine whether protein levels are altered in parallel with gene expression. Rat testis extract and recombinant UNG protein were used as positive controls. Actin was used as a loading control. This experiment is representative of results from 3 different sets of tissue samples from separate litters. ys, yolk sac; emb, embryo.

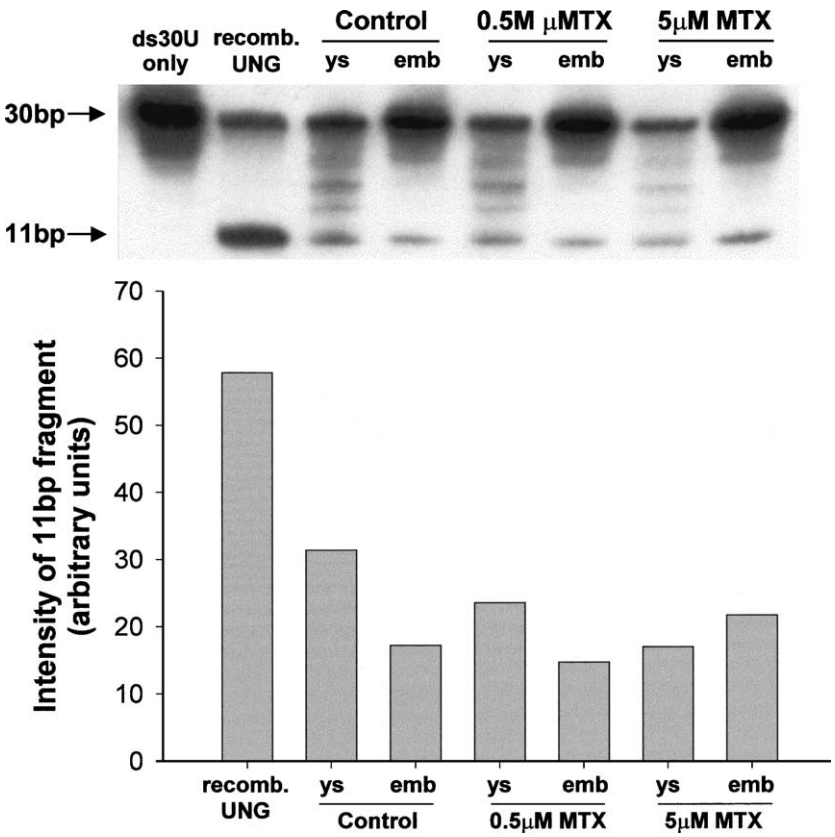

Fig. 9. UNG activity following the culture of GD10 conceptuses with MTX for 6 hr, to determine whether MTX can induce DNA repair activity. Repair reaction products were separated on a 20% denaturing polyacrylamide gel (top photograph). The first lane contains 2 ng ds30U oligonucleotide only. Subsequent lanes are aliquots of reaction samples containing 10 ng ds30U oligonucleotide and: 10 U of each recombinant UNG and APE (recomb. UNG lane) or yolk sac and embryo tissue extracts from conceptuses cultured in the presence of vehicle, 0.5 μM MTX, or 5 μM MTX. A semi-quantitative analysis of the assay is shown below the photograph. Data are represented as the intensity of the 11 bp oligonucleotide band. This experiment is representative of results from 3 different sets of tissue samples from separate litters. ys, yolk sac; emb, embryo.

correlated with the proliferative status of the organ. Another study examining uracil removal activity during neuronal development also demonstrated developmental regulation [43]. The activity profile found in the present study suggests that the yolk sac has predominantly the nuclear form, although the disappearance of the higher-MW protein band on GD12, coupled with the decrease in activity at this time point, argues for decreased ability to remove uracil on GD12 in this tissue. Why UNG protein levels and activity decrease at this time point remains uncertain; increased degradation of UNG may allow for alterations in uracil excision activity independent of increases in protein levels.

Folic acid deficiency has been implicated in the defects induced by exposure to a variety of teratogens, varying from heat shock [44], to methanol [45], or arsenic exposure [46]. The importance of folic acid during development is due to its absolute requirement for the production of DNA nucleotide precursors in all eukaryotic cells; failure to synthesize adequate levels of dTTP results in uracil incorporation into DNA, which can lead to cell death. Deficiency in thymidine biosynthesis during development is a well-known teratogenic condition. This is the first study to examine the regulation of UNG during rat embryo organogenesis *in vivo* and *in vitro* following MTX exposure. We found that culture with MTX induces time- and concentration-dependent malformations *in vitro*. Many of the malformations observed *in vitro* are similar to those found after whole-animal dosing, validating the culture system for examining effects of MTX and the biochemical pathways leading to MTX-induced malformations.

Interestingly, while the rat conceptus modulates *UNG* transcript levels following low-dose MTX, this alteration in transcript levels does not correspond to alterations in protein levels or UNG activity. Curiously, the expression of many other DNA repair genes does not increase during mid-organogenesis; rather, there is sometimes a striking decrease in gene expression following genotoxic teratogen exposure [33,38]. The induction of *UNG* gene expression exclusively following low-dose MTX exposure indicates that this increase is not a general response to genotoxic stress, as presumably there would be as much, and probably much greater, levels of genotoxic stress following high-dose MTX exposure. Perhaps the stress following low-dose MTX exposure is enough to cause activation of damage sensor pathways within the conceptus, whereas

high-dose MTX causes excessive damage, to the extent that cells within the conceptus experience a breakdown in cellular signal and repair pathways.

The presence of high levels of UNG during organogenesis may lead to exacerbation of the genotoxic effects of MTX. A futile repair cycle of excision of uracil from DNA by UNG, and reincorporation of dUTP due to lack of dTTP, leads to DNA strand breaks and cell death (Fig. 1B) [13,47]. The loss of cell viability may contribute to the teratogenicity of MTX. In particular, high UNG activity in the yolk sac may exacerbate the effects of MTX in this tissue, leading to further genomic instability. Of note is the fact that embryos cultured with MTX had much less vasculature and blood cells in the yolk sac; perhaps these cells were killed via thymidineless death. Further studies aimed at modulating UNG activity would shed light on the role of UNG in MTX-induced malformations; *in vivo* inhibition of UNG has not been performed to date due to the nature of the only available inhibitor, UGI, a peptide which must be expressed intracellularly to cause irreversible inhibition [48].

Differences between mitochondrial and nuclear UNG expression following MTX exposure may play a role in the aetiology of MTX-induced malformations. Although several teratogens have been shown to interact with mitochondria via inhibition of energy and respiration pathways [49,50] and induction of oxidative stress [51], none have been shown to induce mitochondrial DNA damage in the conceptus, with the possible exception of diethylstilbestrol [52,53]. Examination of the relative amounts of uracil incorporated into mitochondrial versus nuclear DNA would help determine whether differential genotoxic effects occur following MTX exposure, and whether this effect is related to specific malformations induced by MTX or folic acid deficiency.

The results from this study indicate that the conceptus has a very limited ability to modify the UNG DNA repair pathway in response to MTX; this may indicate susceptibility during this critical window of development to conditions that limit thymidine pools. Factors underlying susceptibility to MTX teratogenicity have been difficult to determine; the results presented in this study show that the conceptus is vulnerable and incapable of modifying key cellular pathways to counteract the MTX insult. While there is a genetic component for a small proportion of NTDs [54–56], studies demonstrate that neither single mutations in critical genes of the folate metabolic pathway nor decreased activity of these enzymes account for the majority of NTDs in infants born to folate-deficient mothers. Therefore, an understanding of the downstream pathways that utilize folate one-carbon pathway products may shed light on the aetiology of NTDs. We suggest that the inability of the embryo to respond to genotoxic stress during development is critical in mediating the malformations that are induced following folic acid deficiency and MTX exposure.

Acknowledgments

We thank H. Krokan for the UNG cDNA, M. Bussemakers for the vimentin cDNA, and G. Slupphaug for the anti-UNG antibody and for his advice on the UNG repair pathway. This study was supported by the Canadian Institute of Health Research and FCAR Québec.

References

[1] Gready JE. Dihydrofolate reductase: binding of substrates and inhibitors and catalytic mechanism. Adv Pharmacol Chemother 1980; 17:37–102.
[2] Hall J, Solehdin F. Folic acid for the prevention of congenital anomalies. Eur J Pediatr 1998;157:445–50.
[3] Campbell LR, Dayton DH, Sohal GS. Neural tube defects: a review of human and animal studies on the etiology of neural tube defects. Teratology 1986;34:171–87.
[4] Copp AJ, Brook FA, Estibeiro JP, Shum ASW, Cockroft DL. The embryonic development of mammalian neural tube defects. Prog Neurobiol 1990;35:363–403.
[5] Berry CL. Transient inhibition of DNA synthesis by methotrexate in the rat embryo and foetus. J Embryol Exp Morphol 1971;26: 469–74.
[6] Darab DJ, Minkiff R, Sciote J, Sulik KK. Pathogenesis of median facial clefts in mice treated with methotrexate. Teratology 1987;36: 77–86.
[7] Jordan RL, Wilson JG, Schumacher HJ. Embryotoxicity of the folate antagonist methotrexate in rats and rabbits. Teratology 1977;15:73–9.
[8] Khera KS. Teratogenicity studies with methotrexate, aminopterin, and acetylsalicylic acid in domestic cats. Teratology 1976;14:21–7.
[9] Milunsky A, Graef JW, Gaynor MF. Methotrexate-induced congenital malformations. J Pediatr 1968;72:790–5.
[10] Warkany J. Aminopterin and methotrexate: folic acid deficiency. Teratology 1978;17:353–8.
[11] Lucock M. Folic acid: nutritional biochemistry, molecular biology, and role in disease processes. Mol Genet Metab 2000;71:121–38.
[12] Kunkel TA, Loeb LA. Fidelity of mammalian DNA polymerases. Science 1981;213:765–7.
[13] Goulian M, Bleile B, Tseng BY. The effect of methotrexate on levels of dUTP in animal cells. J Biol Chem 1980;255:10630–7.
[14] Blount BC, Ames BN. Analysis of uracil in DNA by gas chromatography-mass spectrometry. Anal Biochem 1994;219:195–200.
[15] Pogribny IP, Muskhelishvili L, Miller BJ, James SJ. Presence and consequence of uracil in preneoplastic DNA from folate/methyl-deficient rats. Carcinogenesis 1997;18:2071–6.
[16] Duthie SJ, Grant G, Narayanan S. Increased uracil misincorporation in lymphocytes from folate-deficient rats. Br J Cancer 2000;83:1532–7.
[17] Duthie SJ, Hawdon A. DNA instability (strand breakage, uracil misincorporation, and defective repair) is increased by folic acid depletion in human lymphocytes *in vitro*. FASEB J 1998;12:1491–7.
[18] Seno T, Ayusawa D, Shimizu K, Koyama H, Takeishi K, Hori T. Thymidineless death and genetic events in mammalian cells. Basic Life Sci 1985;31:241–63.
[19] Borchers AH, Kennedy KA, Straw JA. Inhibition of DNA excision repair by methotrexate in Chinese hamster ovary cells following exposure to ultraviolet irradiation or ethylmethanesulfonate. Cancer Res 1990;50:1786–9.
[20] Sutton C, McIvor RS, Vagt M, Doggett B, Kapur RP. Methotrexate-resistant form of dihydrofolate reductase protects transgenic murine embryos from teratogenic effects of methotrexate. Pediatr Dev Pathol 1998;1:503–12.
[21] DeSesso JM, Jordan RL. Drug-induced limb dysplasias in fetal rabbits. Teratology 1977;15:199–212.

[22] Haug T, Skorpen F, Kvaloy K, Eftedal I, Lund H, Krokan HE. Human uracil-DNA glycosylase gene: sequence organization, methylation pattern, and mapping to chromosome 12q23-q24.1. Genomics 1996; 36:408–16.
[23] Nilsen H, Otterlei M, Haug T, Solum K, Nagelhus TA, Skorpen F, Krokan HE. Nuclear and mitochondrial uracil-DNA glycosylases are generated by alternative splicing and transcription from different positions in the *UNG* gene. Nucleic Acids Res 1997;25:750–5.
[24] Nilsen H, Rosewell I, Robins P, Skjelbred CF, Daly G, Krokan HE, Lindahl T, Barnes DE. Uracil-DNA glycosylase (UNG)-deficient mice reveal a primary role of the enzyme during DNA replication. Mol Cell 2000;5:1059–65.
[25] Slupphaug G, Eftedal I, Kavli B, Bharati S, Helle NM, Haug T, Levine DW, Krokan HE. Properties of a recombinant human uracil-DNA glycosylase from the *UNG* gene and evidence that *UNG* encodes the major uracil-DNA glycosylase. Biochemistry 1995;34:128–38.
[26] Pearl LH. Structure and function in the uracil-DNA glycosylase superfamily. Mutat Res 2000;460:165–81.
[27] Haug T, Shorpen F, Aas PA, Malm V, Skjelbred C, Krokan HE. Regulation of expression of nuclear and mitochondrial forms of human uracil-DNA glycosylase. Nucleic Acids Res 1998;26:1449–57.
[28] Weng Y, Sirover MA. Developmental regulation of the base excision repair enzyme uracil DNA glycosylase in the rat. Mutat Res 1993;293:133–41.
[29] Nilsen H, Steinsbekk KS, Otterlei M, Slupphaug G, Aas PA, Krokan HE. Analysis of uracil-DNA glycosylases from the murine *Ung* gene reveals differential expression in tissues and in embryonic development and a subcellular sorting pattern that differs from the human homologues. Nucleic Acids Res 2000;28:2277–85.
[30] New DAT. Whole embryo culture and the study of mammalian embryos during organogenesis. Biol Rev 1978;53:81–112.
[31] van Gelder RN, von Zastrow ME, Yool A, Dement WC, Barchas JD, Eberwine JH. Amplified RNA synthesized from limited quantities of heterogeneous cDNA. Proc Natl Acad Sci USA 1990;87:1663–7.
[32] Taylor LE, Bennett GD, Finnell RH. Altered gene expression in murine branchial arches following in utero exposure to retinoic acid. J Craniofac Genet Dev Biol 1995;15:13–25.
[33] Vinson RK, Hales BF. Nucleotide excision repair gene expression in the rat conceptus during organogenesis. Mutat Res 2001;486:113–23.
[34] Hallick RB, Chelm BK, Gray PW, Orozco Jr EM. Use of aurintricarboxylic acid as an inhibitor of nucleases during nucleic acid isolation. Nucleic Acids Res 1977;4:3055–64.
[35] Gonzalez RG, Haxo RS, Schleich T. Mechanism of action of polymeric aurintricarboxylic acid, a potent inhibitor of protein-nucleic acid interactions. Biochemistry 1980;19:4299–303.
[36] Wang ZG, Smith DG, Mosbaugh DW. Overproduction and characterization of the uracil-DNA glycosylase inhibitor of bacteriophage PBS2. Gene 1991;99:31–7.
[37] Brown NA, Fabro S. Quantitation of rat embryonic development in vitro: a morphological scoring system. Teratology 1981;24:65–78.
[38] Vinson RK, Hales BF. Expression of base excision, mismatch, and recombination repair genes in the organogenesis-stage rat conceptus and effects of exposure to a genotoxic teratogen, 4-hydroperoxycyclophosphamide. Teratology 2001;64:283–91.
[39] Wilkinson KD. Ubiquitination and deubiquitination: targeting of proteins for degradation by the proteasome. Semin Cell Dev Biol 2000;11:141–8.
[40] Vilpo JA. The DNA-repair enzyme uracil-DNA glycosylase in the human hematopoietic system. Mutat Res 1988;193:207–17.
[41] Hromas R, Collins SJ, Hickstein D, Raskind W, Deaven LL, O'Hara P, Hagen FS, Kaushansky K. A retinoic acid-responsive human zinc finger gene, *MZF-1*, preferentially expressed in myeloid cells. J Biol Chem 1991;266:14183–7.
[42] Palis J, Yoder MC. Yolk-sac hematopoiesis: the first blood cells of mouse and man. Exp Hematol 2001;29:927–36.
[43] Focher F, Mazzarello P, Verri A, Hubscher U, Spaderi S. Activity profiles of enzymes that control the uracil incorporation into DNA during neuronal development. Mutat Res 1990;237:65–73.
[44] Shin JH, Shiota K. Folic acid supplementation of pregnant mice suppresses heat-induced neural tube defects in the offspring. J Nutr 1999;129:2070–3.
[45] Sakanashi TM, Rogers JM, Fu SS, Connelly LE, Keen CL. Influence of maternal folate status on the developmental toxicity of methanol in the CD-1 mouse. Teratology 1996;54:198–206.
[46] Ruan Y, Peterson MH, Wauson EM, Waes JG, Finnell RH, Vorce RL. Folic acid protects SWV/Fnn embryo fibroblasts against arsenic toxicity. Toxicol Lett 2000;117:129–37.
[47] Goulian M, Bleile B, Tseng BY. Methotrexate-induced misincorporation of uracil into DNA. Proc Natl Acad Sci USA 1980;77:1956–60.
[48] Radany EH, Dornfeld KJ, Sanderson RJ, Savage MK, Majumdar A, Seidman MM, Mosbaugh DW. Increased spontaneous mutation frequency in human cells expressing the phage PBS2-encoded inhibitor of uracil-DNA glycosylase. Mutat Res 2000;461:41–58.
[49] Mackler B, Grace R, Tippit DF, Lemire RJ, Shepard TH, Kelley VC. Studies of the development of congenital anomalies in rats. III. Effects of inhibition of mitochondrial energy systems on embryonic development. Teratology 1975;12:291–6.
[50] Ranganathan S, Churchill PF, Hood RD. Inhibition of mitochondrial respiration by cationic rhodamines as a possible teratogenicity mechanism. Toxicol Appl Pharmacol 1989;99:81–9.
[51] Liu L, Wells PG. *In vivo* phenytoin-initiated oxidative damage to proteins and lipids in murine maternal hepatic and embryonic tissue organelles: potential molecular targets of chemical teratogenesis. Toxicol Appl Pharmacol 1994;125:247–55.
[52] Beyer BK, Greenaway JC, Fantel AG, Juchau MR. Embryotoxicity induced by diethylstilbestrol in vitro. J Biochem Toxicol 1987;2: 77–92.
[53] Thomas RD, Roy D. Mitochondrial enzyme-catalyzed oxidation and reduction reactions of stilbene estrogen. Carcinogenesis 1995;16:891–5.
[54] Papapetrou C, Lynch SA, Burn J, Edwards YH. Methylenetetrahydrofolate reductase and neural tube defects. Lancet 1996;348:348–58.
[55] Shaw GM, Rozen R, Finnell RH, Wasserman CR, Lammer EJ. Maternal vitamin use, genetic variation of infant methylenetetrahydrofolate reductase, and risk for spina bifida. Am J Epidemiol 1998; 148:30–7.
[56] Barber RC, Lammer EJ, Shaw GM, Greer KA, Finnell RH. The role of folate transport and metabolism in neural tube defect risk. Mol Genet Metab 1999;66:1–9.